ACS Sustainable Chemistry & Engineering

Research Article

pubs.acs.org/journal/ascecg

Rheologically Determined Critical Shear Rates for Shear-Induced Nucleation Rate Enhancements of Poly(lactic acid)

Yong Zhong, Huagao Fang, Yaqiong Zhang, Zhongkai Wang, Jingjing Yang, and Zhigang Wang*

CAS Key Laboratory of Soft Matter Chemistry, Department of Polymer Science and Engineering, Hefei National Laboratory for Physical Sciences at the Microscale, University of Science and Technology of China, Hefei, Anhui Province 230026, P. R. China

ABSTRACT: Both the nonisothermal and isothermal crystallization kinetics under the influences of different shear conditions for poly(lactic acid) (PLA) were investigated by rheometry. The nucleation and growth of PLA spherulites during isothermal crystallization with different shear conditions were observed by polarized optical microscopy (POM). Shear-induced nucleation rate enhancements of PLA were studied on the basis of the prerequisite determination of the critical shear rates, for which the stretch of the longest chains (high molecular mass tails) of PLA would be expected. The transitions between different shear flow regimes for shear-induced crystallization of PLA at the temperature of 135 °C were determined by two characteristic Weissenberg numbers on the basis of reptation time and Rouse time for the high molecular mass tails, which were determined through combination of the discrete Maxwell relaxation time spectra of PLA at the reference temperature of 190 °C and the Arrhenius type of temperature dependence for the horizontal shift factor, a_T. It was then found that the crystallization process of PLA was greatly enhanced by shear compared to the quiescent condition, and the crystallization kinetics could be accelerated by the increased shear rate and/or shear time. It was more interesting to find that there existed a critical shear time under a certain shear rate, and a further increase in the shear time did not lead to further acceleration of the crystallization kinetics. POM observation indicated that the acceleration of crystallization kinetics was obviously brought about by the enhanced nucleus density under the application of shear and the subsequent spherulitic growth rates kept about constant. Thus, a kinetic model based on directly relating the extra number of activated nuclei promoted by shear to the shear rate was further applied to well predict the effects of shear time on the shear-induced isothermal crystallization kinetics of PLA.

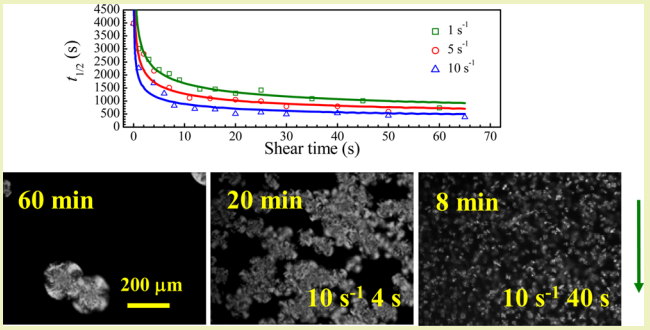

KEYWORDS: *Poly(lactic acid), Nucleation, Spherulite, Crystallization, Shear, Rheology*

INTRODUCTION

The vast majority of existing polymer materials, notably poly(vinyl chloride) and polyolefins, are made from nonrenewable fossil resources, which will be eventually extinguished. In addition, both the manufacture of these synthetic polymers and their disposal by incineration produce CO_2, which contributes to global warming. Consequently, there is a need to develop new synthetic polymers based on renewable resources due to the pressing environmental and economic concerns. For this reason, poly(lactic acid) (PLA) received great attention in recent years because of its biodegradation, biocompatibility, and appropriate mechanical properties.[1−9] PLA can be synthesized from a renewable agricultural resource (corn) and can easily degrade through simple hydrolysis. Although PLA has been traditionally used for biomedical applications such as implant devices, tissue scaffolds, and internal sutures, PLA has now rapidly gained recognition as an important biodegradable thermoplastic in the medical, agricultural, and general purpose plastic fields because the reasonably good optical, physical, mechanical, and barrier properties of PLA can be well compared to that of existing petroleum-based polymers.[10−15]

However, because of the slow crystallization rate, the PLA products often exhibit an amorphous state, resulting in relatively poor physical properties such as poor dimensional accuracy and stability and low modulus and strength, which consequently limits its practical applications, and various chemical modification and blending methods were used to improve the physical properties of PLA.[11] Understanding the crystallization behavior of PLA is crucial to controlling its microstructure and providing guidance for industrial processing conditions. To date, many efforts have been devoted to investigating the crystallization kinetics and crystalline morphologies of PLA under different conditions.[16−23] However, these crystallization studies were mostly carried out under quiescent crystallization conditions, which avoided the influences of different levels of flow field such as elongation,

Received: February 14, 2013
Revised: March 22, 2013
Published: April 9, 2013

shear or mixed elongation, and shear subjected on the molten PLA for the factual polymer processing such as injection molding and fiber spinning. With respect to the effects of flow field on the crystallization behaviors of polymers, most of the studies usually selected isotactic polypropylene (*i*PP) and polyethylene (PE) as the materials, and the results showed that flow field can drastically enhance the crystallization kinetics, mainly through an acceleration of the nucleation process.[24−27] At the appropriate shear conditions, the crystalline morphologies can be altered from the spherulites to a shish-kebab structure.[25−34] Unlike flexible chain polymers such as PE and *i*PP, PLA might exhibit different shear-induced crystallization kinetics and crystalline morphologies, which is mainly due to the nature of semi-rigid and stereocomplex chain structures for PLA.[35] Obviously, for PLA to be adapted at a wide scale for uses as a conventional thermoplastic, the subject on crystallization behaviors of PLA under flow field has the practical significance for guiding its forming and processing. Despite this crucial need, only sparse studies on the effects of shear flow on PLA crystallization were reported in the literature, and these studies mainly focused on the shear-induced crystalline morphologies of PLA.[35−43] For examples, Fitz et al. found that the step shear at the condition of shear rate of 1 s^{-1}, shear strain of 125%, and shear time of 1 s does not affect any of the crystalline morphology of PLA.[36] Mahendrasingam et al. found that the shish-kebab crystalline morphology of PLA forms during rapid tensile deformation.[37] The formation of PLA fibrillar crystals is relevant to the flow fields that exist in the fiber spinning processing.[38,39] Li et al. recently studied the steady shear-induced isothermal crystallization (with a single shear rate of 1 s^{-1} below 140 °C)[40] and nonisothermal crystallization of PLA under quiescent and steady shear conditions (with three shear rates of 4, 5, and 6 s^{-1} at slow cooling rates below 5 °C/min)[41] by using polarized optical microscopy equipped with a shear hot stage and off-line wide-angle X-ray diffraction technique, which demonstrated that both the shear rate and cooling rate play significant roles on the final crystalline morphologies and crystallinities of PLA. Yamazaki et al. recently reported steady shear-induced isothermal crystallization of PLA (with a single shear rate of 5 s^{-1} mostly at temperatures higher than 140 °C),[42] in which the "shish-like" fibril crystals were observed by polarized optical microscopy, SEM, and small-angle X-ray scattering (SAXS). Huang et al. recently reported the crystalline structure, morphology, and melting behavior of PLA under shear conditions by wide-angle X-ray diffraction (WAXD), differential scanning calorimetry (DSC), and in situ polarized optical microscopy (POM),[43] in which cylindric morphology with arranged spherulites was observed in PLA films at high crystallization temperature (T_c) under application of shear. However, it is clearly concerned that overall there is a lack of systematic investigation on the relationship between the chosen shear conditions and crystallization kinetics for the PLA material, which is definitely vital to understanding the crystallization behaviors of PLA for processing, compared with the extensive shear-induced crystallization studies on other thermoplastics such as *i*PP, PE, and their blends or composites.[25−29,31−34]

The aim of the present work was to investigate the shear effects on the crystallization kinetics of PLA under non-isothermal and isothermal crystallization conditions. The first most important issue to be resolved before any further studies was to determine appropriate shear conditions. Therefore, the rheological properties of PLA melts were comprehensively investigated at first. Then, the transitions between different shear flow regimes defined by two characteristic Weissenberg numbers could be determined. With shear rates determined, at which the longest chains (high molecular mass tails) of PLA were expected to be stretched, the influences of combination of shear rate and shear time on the changes of crystallization kinetics and on the morphological evolutions of PLA were studied by rheometry and in situ POM. Finally, a kinetic model based on directly relating the extra number of activated nuclei created during shear to shear rate was used to well predict the effects of shear rate and shear time on the shear-induced isothermal crystallization kinetics of PLA.

EXPERIMENTAL SECTION

Material and Preparation of Samples. Poly(lactic acid) (trade name 4032D, NatureWorks China/Hong Kong, Shanghai, China) used in this study was a commercial product with 98.7 mol % L-isomeric content in granular pellet form, density of 1.24 g/cm^3, weight-average molecular mass of 160 kg/mol, and polydispersity of 1.67 (the latter two values were measured by using Waters 2414 GPC, Waters Corporation, U.S.A.). The nominal melting point and glass transition temperature determined by differential scanning calorimetry (DSC) were 164.5 and 56 °C, respectively. The as-received granular pellets were compression molded at 180 °C for 5 min in a homemade laboratory vacuum hot presser to obtain disk-shaped samples having diameters of 25 mm and thicknesses of approximately 1.0 mm. Before compression molding, the as-received granular pellets were dried in a vacuum oven at 50 °C for at least 24 h to remove moisture for reducing the possibility of hydrolytic degradation of PLA. After compression molding, the disk-shaped samples were further dried in vacuum at 60 °C for 6 h before the rheological measurements.

Measurements on Rheological Properties. The linear viscoelastic regime for PLA melts was measured by using a stress-controlled rheometer (TA-AR2000EX, TA Instruments, U.S.A.) with 25 mm plate−plate geometry. To determine the linear viscoelastic regime, a strain sweep with a fixed frequency of 6.28 rad/s was performed. The chosen strain of 5% fell well within the linear viscoelastic regime at all the used temperatures. The small amplitude oscillatory sweeps were performed over a wide range of temperatures from 170 to 210 °C and angular frequencies from 0.2 to 500 rad/s. Measurements were performed by starting at the highest frequency (500 rad/s) and stepping to the lowest one (0.2 rad/s). All the rheological experiments were performed in nitrogen atmosphere to avoid possible sample degradation. The time−temperature superposition principle was applied to obtain the mastercurves for PLA at the reference temperature of 190 °C.

Measurements on Shear-Induced Crystallization Kinetics. A rheometer was used to measure the crystallization kinetics of PLA under quiescent conditions and after the shear application, respectively, for both nonisothermal and isothermal crystallization processes. This widely used experimental technique combined the possibility of applying shear and subsequently measuring the mechanical spectrum to track the crystallization process of polymers from melts because the linear viscoelastic material functions were sensitive to the structural changes of the undercooled polymer melts. Generally, the crystallization process was monitored through the response of the sample to a low enough oscillatory strain at a fixed frequency. It must be emphasized that the imposed strain must be low enough not to influence the crystallization kinetics and not to damage the samples. Thus, a much lower strain of 0.1% was adapted to avoid the crystallization kinetics to be modified. During the crystallization process, the sample usually experienced a contraction, which induced an obvious variation of the sample dimension. Because of the dimensional change, the sample was subjected to a large longitudinal force, which might cause errors on the measurements of the storage modulus. In order to keep the force value at zero, the gap between the parallel plates was automatically adjusted throughout the crystallization

process according to the normal force transducer of the rheometer. The experimental procedure for the shear-induced crystallization is shown in Figure 1 and is described as follows: First, a disk-shaped PLA

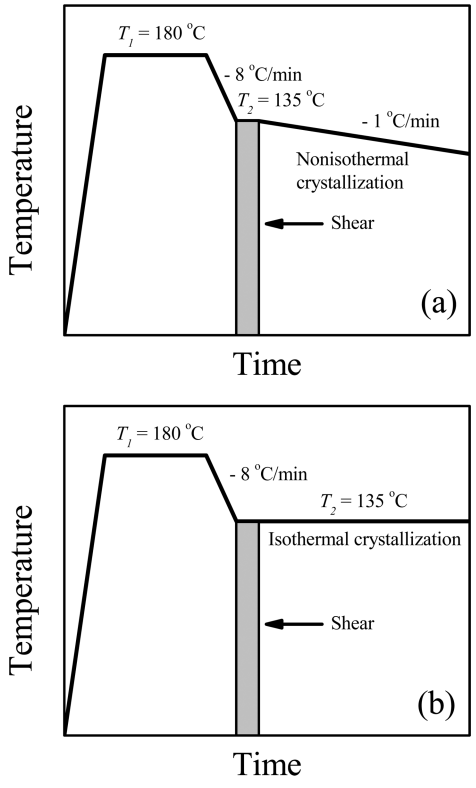

Figure 1. Schematic indications of thermal and shear applications for (a) nonisothermal crystallization process and (b) isothermal crystallization process for PLA.

sample was loaded at the temperature of 180 °C (T_1) and held for 10 min to erase the thermal history. Subsequently, the PLA sample was cooled as fast as possible (−8 °C/min) to the desired crystallization temperature of 135 °C (T_2), and then a precisely controlled step shear treatment programmed as a preshear option in the usual time−temperature sweep experiment was applied to the undercooled melt. For the nonisothermal crystallization process, a temperature sweep at a cooling rate of 1 °C/min from 135 to 70 °C was performed at an angular frequency of 1 rad/s to trace the evolution of storage modulus of PLA with temperature (Figure 1a). For the isothermal crystallization process at T_2, a time sweep at an angular frequency of 1 rad/s was performed to trace the evolution of storage modulus of PLA with time until the crystallization process was completed (Figure 1b).

Shear-Induced Morphological Evolutions for PLA Observed by POM. The nucleation and growth of spherulites for PLA film samples during the isothermal crystallization process under the application of shear were observed by using a polarized optical microscopy (Olympus BX51, Japan) equipped with a high-temperature optical shear hot stage (Linkam CSS-450, UK). The gap between the two glass windows in the shear hot stage was set at 10 μm. The PLA film samples were melted at 180 °C for 10 min to eliminate thermal history and then cooled to the isothermal crystallization temperature of 135 °C at a rate of 8 °C/min. Once the temperature reached 135 °C, steady shears with different selective shear rates or shear times were immediately applied to PLA melts to examine the changes of nucleation and growth rate of PLA spherulites with the shear conditions by continuously taking the optical micrographs at appropriate time intervals just after shear cessation until impingements of the growing spherulites. In order to avoid the effect of PLA thermal degradation, for each measurement a fresh PLA film sample was used.

RESULTS AND DISCUSSION

Determination of the Critical Shear Rates by Rheological Classification. The shear-induced crystallization behaviors are closely related to the rheological properties of polymer melts. Their interactions were well interpreted in the literature by defining the four different flow regimes on the basis of rheology of polymers.[44] The transitions between these regimes are characterized by critical values of the Weissenberg number (Wi). In Regime I, for $Wi_{rep} < 1$ and $Wi_s < 1$, the polymer chains are in their equilibrium state, thus, shear flow has no effects on crystallization. Generally, polymer chains tend to be oriented for $Wi_{rep} > 1$ and $Wi_s < 1$ (Regime II), to be stretched for $Wi_s > 1$ (Regime III), and in Regime IV, the polymer chains are strongly stretched for a sufficient time to fulfill the condition that the molecular stretch ratio, λ, is larger than a critical value, $\lambda^*(T)$. Regime II is necessary for the enhancement of the number density of the activated nuclei, and Regime III ensures sufficient stretch of the polymer chains into a conformation ideal for the formation of oriented nuclei. These transitions suggest that there is a minimum shear rate ($1/\tau_R$), below which the oriented nuclei cannot be obtained, and therefore, the shish-kebab crystalline morphology is unlikely to be observed for such a crystallized polymer.

In order to determine the critical shear rate (reciprocal of the Rouse time, τ_R) for PLA, dynamic frequency sweep measurements were performed at five temperatures above the nominal melting point of PLA (164.5 °C). Figure 2 shows the changes

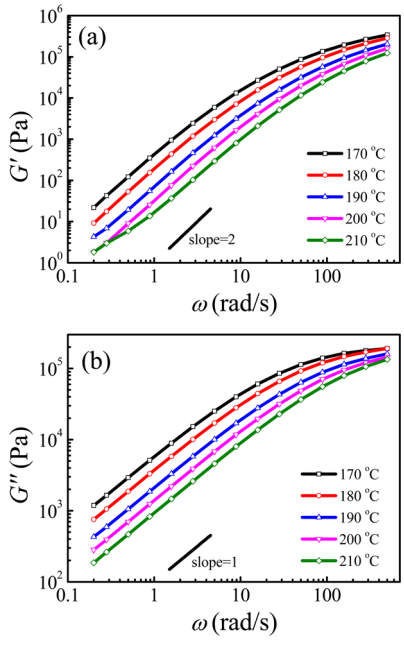

Figure 2. Changes of (a) storage modulus, G', and (b) loss modulus, G'', as functions of angular frequency, ω, at different temperatures for PLA.

of storage modulus, G', and loss modulus, G'', with angular frequency, ω, for PLA melts at the temperatures between 170 and 210 °C. As expected, the moduli of PLA melts decrease with increasing temperature. At low frequencies, PLA chains are fully relaxed, and PLA exhibits the typical terminal behavior with the scaling laws of about $G' \propto \omega^2$ and $G'' \propto \omega$. It should be noticed that at the highest applied temperature of 210 °C and at frequencies lower than 1 rad/s, G' values show a slight

dx.doi.org/10.1021/sc400040b | ACS Sustainable Chem. Eng. 2013, 1, 663−672

deviation from the terminal slope. Such a deviation is the signature of the relatively fast chemical degradation of PLA chains at this high temperature.[45]

By applying the time−temperature superposition principle, the mastercurves for PLA can be constructed. Figure 3 shows

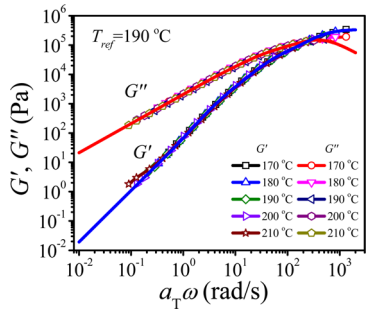

Figure 3. Mastercurves of storage modulus, G', and loss modulus, G'', versus the reduced angular frequency, $a_T\omega$ at the reference temperature, T_{ref} of 190 °C for PLA. The solids lines are obtained from the discrete Maxwell relaxation time spectra.

the mastercurves of storage and loss moduli referenced to the temperature of 190 °C, which are constructed from the five isothermal frequency sweep curves as shown in Figure 2. The vertical shift factor of unity ($b_T = 1$) is taken, and the horizontal shift factors, a_T, are obtained on the basis of the reference temperature.[46] To quantify the temperature dependence of viscoelastic properties of PLA, the horizontal shift factors, a_T, at different temperatures are fitted by using the Arrhenius equation as follow

$$\log a_T = \frac{E_a}{2.303R}\left(\frac{1}{T} - \frac{1}{T_{ref}}\right) \quad (1)$$

where R is the universal gas constant, E_a is the activation energy for flow, T is the measurement temperature, and T_{ref} is the reference temperature. The fitting result is shown in Figure 4

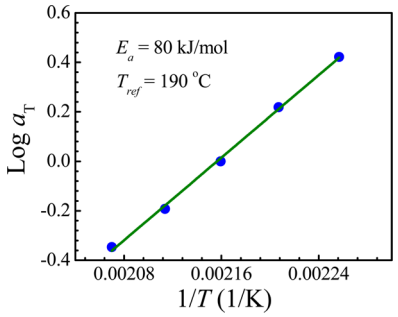

Figure 4. Change of the horizontal shift factor, a_T versus $1/T$ at the reference temperature T_{ref} of 190 °C for PLA.

with the activation energy of flow determined to be E_a = 80 kJ/mol. This E_a value is well comparable with the reported E_a of about 79 kJ/mol for PLA with a close weight-average molecular mass of 130 kg/mol in the literature.[46]

The constructed mastercurves for PLA can be described by using the discrete Maxwell relaxation time spectra (G_i, τ_i)[47]

$$G'(\omega) = \sum_{i=1}^{N} \frac{G_i\omega^2\tau_i^2}{1 + \omega^2\tau_i^2} \quad (2)$$

$$G''(\omega) = \sum_{i=1}^{N} \frac{G_i\omega\tau_i}{1 + \omega^2\tau_i^2} \quad (3)$$

where G_i is the modulus corresponding to the relaxation time, τ_i. The parameters G_i and τ_i were obtained by calculating from the G' and G'' data by using the standard nonlinear regression method in Trios Software (TA Instruments, U.S.A.). Five modes were applied to fit the G' and G'' data according to the common rule, which was 1.2−1.5 modes per decade in frequency ω.[48] The best sets of the modulus, G_i, and relaxation time, τ_i, are listed in Table 1, which can be used to nicely fit the measured G' and G'' data (see the solid lines shown in Figure 3).

Table 1. Relaxation Spectra, G_i and τ_i, Obtained from Linear Viscoelastic Data for PLA Melts at Reference Temperature, T_{ref} of 190 °C

mode	$G_i \times 10^{-5}$ (Pa)	τ_i (s)
1	2.808	0.00253
2	0.3387	0.01285
3	0.251	0.02615
4	0.02184	0.1388
5	0.00002	7.905

On the basis of the analyses of the shear-induced crystallization studies reported in the literature, it is concluded that the stretch of the longest chains (high molecular mass tails, HMW tails) of polymers dominates the dynamics of the shear-induced crystallization.[27,28,49−52] Thus, the longest relaxation time from the relaxation spectra is used as a measure of the HMW tails. The Rouse time (stretch relaxation time), τ_R of PLA can be calculated using the relation based on the tube model of Doi and Edwards[53]

$$\tau_R = \tau_{rep}/3Z \quad (4)$$

where Z is the average number of entanglements ($Z = M_w/M_e$, M_e is the molecular mass between entanglements). The calculated Z value for PLA is 20 by using the M_e value of 8000 g/mol for PLA.[46] Table 2 lists the longest relaxation times

Table 2. Longest Reptation time (τ_{rep}^{HMW}) and Rouse Time (τ_R^{HMW}) Determined from Relaxation Spectra and Corresponding Critical Shear Rates for the Orientation Stretch Regime Transition

T (°C)	$\tau_{rep}^{HMW}(s)$	$\tau_R^{HMW}(s)$	$\dot{\gamma}_{I\to II}(s^{-1})^a$	$\dot{\gamma}_{II\to III}(s^{-1})^a$
190	7.9	0.132	0.127	7.6
135	131	2.2	0.0076	0.45

[a] $\dot{\gamma}_{I\to II}$ and $\dot{\gamma}_{II\to III}$ are critical values of the shear rate for the transition of flow regimes for PLA between regime I and II and regime II and III, respectively.

together with the characteristic shear rates for the transitions between the orientation and stretch regimes for PLA at 190 and 135 °C, respectively. The relaxation times and corresponding characteristic shear rates at 135 °C were calculated using the Arrhenius type of temperature dependence, from which the shear conditions for studying the shear-induced crystallization kinetics of PLA could be chosen. In the followed shear-induced crystallization measurements, the shear rates were set as high as

dx.doi.org/10.1021/sc400040b | ACS Sustainable Chem. Eng. 2013, 1, 663−672

to guarantee $Wi_s > 1$, at which the stretch of the longest chains (high molecular mass tails) of PLA is expected.[54]

Nonisothermal Crystallization of PLA with Shear. The nonisothermal crystallization of PLA under the quiescent condition was examined using the rheometer at first. Figure 5a shows the change of storage modulus, G', during the temperature sweep at the cooling rate of 1 °C/min for PLA. At first G' starts to increase smoothly with decreasing temperature following a straight line on the semilog plot. When the temperature reaches to 121 °C, a slight upturn of G' is observed indicating that the nucleation of PLA sets in. We define this inflection point of G' as the temperature at which crystallization starts ($T_{c,start}$). Subsequently, G' increases rapidly with further decreasing temperature until it reaches a plateau at the temperature of 93 °C. Further cooling does not lead to an obvious increase of G'. We define the second inflection point of G' as the temperature at which crystallization completes ($T_{c,com}$). For comparison, Figure 5b shows the DSC heat flow curve during the cooling scan with the procedure matching the temperature sweep to track dynamic moduli as above described. Note that there are two exothermal peaks (at about 112 and 103 °C, respectively) in the DSC cooling curve, which are associated with two maximum crystallization rates for PLA during cooling at the relatively slow cooling rate of 1 °C/min. At the high temperature, the PLA chain segment mobility is relatively high, thus the growth of PLA spherulites is dominant. When temperature further decreases, the increasing PLA melt viscosity retards the PLA chain segment rearrangements into the growth fronts of PLA spherulites; thus, the growth rate of PLA spherulites decreases. However, when temperature continues to decrease, nucleation becomes a dominant effect on the crystallization kinetics, which results in the second exothermal peak. The starting and end points of the exothermic peak on the heat flow curve are illustrated in Figure 5b, which appear to correspond quite well to the inflection points of G' versus the temperature curve as indicated by the vertical dashed lines. This correspondence demonstrates that the rheometer can be applied to successfully trace the nonisothermal crystallization process of PLA.

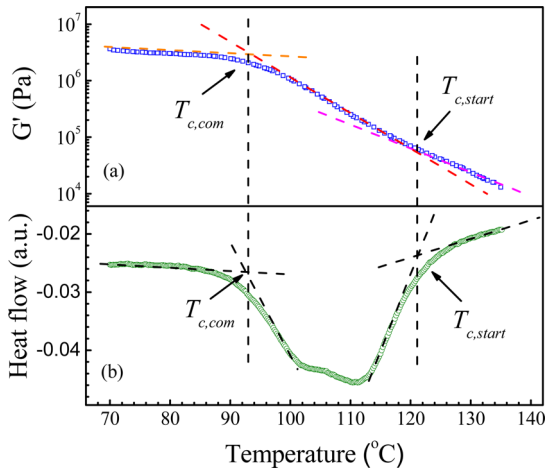

Figure 5. Comparison between two types of temperature sweep tests for PLA (a) change of storage modulus with decreasing temperature during cooling at the cooling rate of 1 °C/min and (b) DSC heat flow curve during cooling at the cooling rate of 1 °C/min.

Then for the applied shear conditions, Figure 6 shows the changes of storage modulus, G', as functions of temperature during cooling at the cooling rate of 1 °C/min from 145 to 70 °C for the PLA samples that were sheared at the temperature of 135 °C with a shear rate of 10 s^{-1} for different shear times, t_s. Note that the Wi_s of 22 is much higher than 1, for which the stretch of the longest chains (high molecular mass tails) of PLA is predicted. It can be found that the shear obviously accelerates the nonisothermal crystallization process of PLA. Under quiescent conditions, the upturn of G' takes place at a much lower temperature of 121 °C as above mentioned; however, G' rises rapidly at 135 °C immediately after shear, no matter how long the shear time is applied. The early onset of crystallization in the presence of shear indicates that shear can drastically enhance of the nucleation process of PLA. It is also evident that the slope of the subsequent buildup of G' after shear increases with increasing shear time until it reaches a maximum at the shear time t_s of 8 s. In order to quantitatively indicate the effect of shear time on the nonisothermal crystallization process of PLA, the change of temperature at which the crystallization completes ($T_{c,com}$) as a function of shear time is shown in Figure 7. For PLA sheared at the shear rate of 10 s^{-1}, $T_{c,com}$ increases with shear time and then tends to saturate. At t_s of 8 s, a plateau value of about 115 °C is approached. Application of a longer shear time is likely to yield only a tiny increase in $T_{c,com}$.

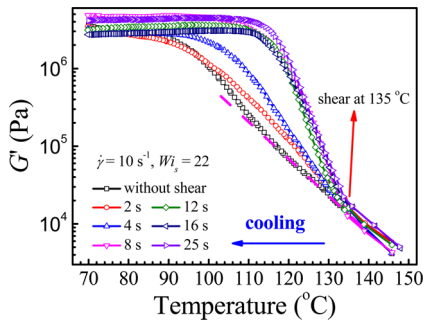

Figure 6. Changes of storage modulus, G', with decreasing temperature for PLA during cooling at the cooling rate of 1 °C/min under the quiescent condition and with shear rate of 10 s^{-1} applied for different shear times at 135 °C.

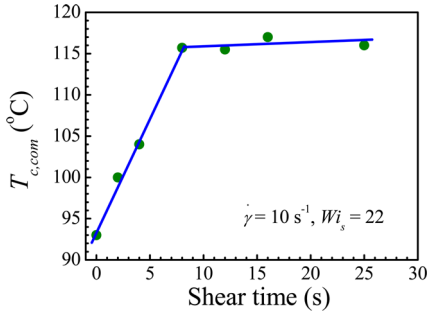

Figure 7. Change of $T_{c,com}$, defined as the temperature at which crystallization is completed, as a function of shear time at the shear rate of $\dot{\gamma}$ = 10 s^{-1} and Wi_s = 22 for PLA.

Shear-Induced Isothermal Crystallization of PLA. Figure 8 shows the evolutions of storage modulus, G', measured during the shear-induced isothermal crystallization of PLA at the temperature of 135 °C after controlled shear at

dx.doi.org/10.1021/sc400040b | ACS Sustainable Chem. Eng. 2013, 1, 663−672

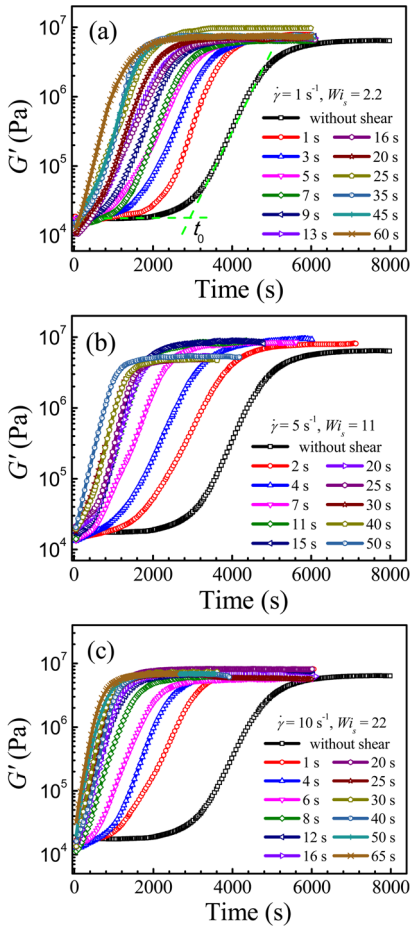

Figure 8. Changes of storage modulus, G', with time during crystallization at T_c of 135 °C for PLA under the quiescent condition and different shear conditions of (a) $\dot{\gamma}$ = 1 s^{-1}, Wi_s = 2.2; (b) $\dot{\gamma}$ = 5 s^{-1}, Wi_s = 11; and (c) $\dot{\gamma}$ = 10 s^{-1}, Wi_s = 22.

135 °C with various fixed shear rates ($\dot{\gamma}$ = 1, 5, and 10 s^{-1}) associated with different shear time, t_s, respectively. Note that the corresponding Wi_s values are larger than 1, for which the stretch of the longest chains (high molecular mass tails) of PLA is predicted. The data for the quiescent crystallization process is plotted in Figure 8 for the comparison purpose. For the quiescent isothermal crystallization process, with the nucleation and growth of spherulites of PLA from the melt, the change of storage modulus, G', with time shows a sigmoidal shape, exhibiting a progression of storage modulus from about constant values before the start of crystallization to a rapid increase and then approaching the plateau values at the ending of the primary crystallization stage. The time at the intersection of the highest slope of the storage modulus−time curve with the line through the initial constant storage modulus values (indicated by the green dashed lines in Figure 8a) is often defined as the induction time, t_0 for crystallization.[55] At the temperature of 135 °C, the induction time needed for the onset of crystallization of PLA is about 2900 s. When a shear is applied, the storage modulus curve shifts to the shorter time region, and the induction time is significantly reduced with increasing shear time in comparison with the quiescent condition, indicating an acceleration of the crystallization kinetics. At the applied shear rate and shear time, the initial storage modulus exhibits an immediate increase, indicating an instantaneous nucleation for crystallization due to the shear effect except for the t_s of 1 s condition. However, the shift becomes less obvious at the sufficiently longer shear times, which implies that the acceleration of crystallization kinetics by shear can become saturated after a certain shear time. The shortening of the induction time for crystallization is a signature of formation of extra nuclei activated by shear, which will be discussed more in the later section. It should be pointed out that the plateau values for G' at the end of the primary crystallization stage show some variations among the curves probably due to slight differences in the sample position between the parallel plates of the rheometer and due to the fluctuations in the gap distance, which influence the sample diameters. Note that the contact states of the solidified PLA samples within the geometry in individual measurements are different from each other because the shrinkages of PLA samples within the geometry during the crystallization processes cannot be exactly identical.

Although the above dynamic mechanical spectroscopy provides a reliable tool to follow the crystallization process of polymers from the melts, the interrelation between the transformed fraction of melt to crystallites and the mechanical data is not so simple.[56] However, for simplicity, a logarithmic normalization of the G' data is used to applying for an estimation of the transformed fraction (relative crystallinity, $x(t)$) by following that Pogodina et al. have proposed as follow[57]

$$x(t) = \frac{\log G'(t) - \log G'_{\min}}{\log G'_{\max} - \log G'_{\min}} \quad (5)$$

where $G'_{\min}$ and $G'_{\max}$ are the values of the starting storage modulus and ending plateau storage modulus, respectively. Then, the influences of shear on the isothermal crystallization kinetics of PLA can be simply quantified by defining the crystallization half time, $t_{1/2}$, at which half of the change in the viscoelastic functions occurs.[48] The changes of relative crystallinity with time during crystallization at T_c of 135 °C for PLA under the quiescent condition and different shear conditions are shown in Figure 9. The influences of shear time at different shear rates on the crystallization half time, $t_{1/2}$, are shown in Figure 13. It can be clearly seen that the crystallization half time decreases rapidly as soon as the shear is applied, followed by a region where the crystallization half time is almost unaffected by the further increased shear time. The crystallization half time for PLA at the quiescent condition is 3980 s, while with a shear rate of 10 s^{-1} for 4 s, the crystallization half time of PLA reduces to 1690 s. At the shear time of around 8 s, the crystallization half time starts to saturate. This result is in agreement with the shear-induced nonisothermal crystallization. The crystallization half time also decreases with the increased shear rate. For an instance, the crystallization half times of PLA sheared at the shear rates of 1 s^{-1} and 10 s^{-1} for the same shear time of 1 s are 3010 and 2260 s, respectively.

Shear-Induced Nucleation and Growth of PLA Spherulites. The effects of shear flow with shear rates of 1, 5, and 10 s^{-1}, respectively, on morphological evolutions of PLA during isothermal crystallization were studied by using polarized optical microscopy. Figure 10 shows the nucleation and growth of PLA spherulites during isothermal crystallization at T_c of 135 °C after the PLA samples were subjected to shear at a shear rate of 10 s^{-1} for different shear times (for the quiescent condition, see the micrographs in panel A). It can be

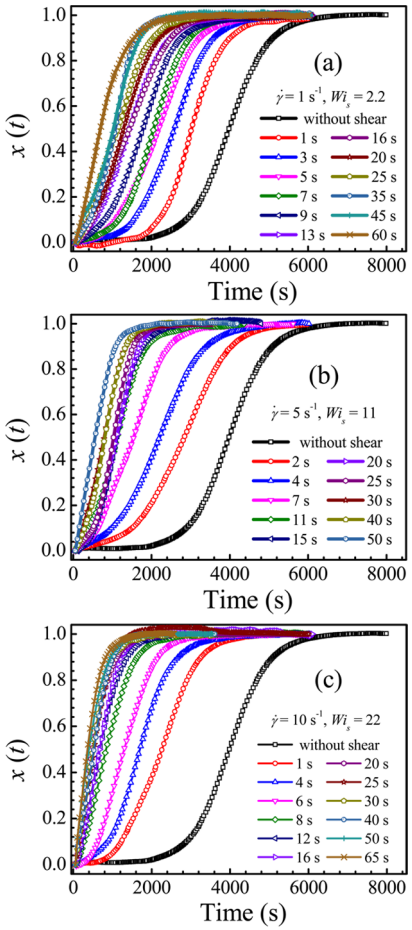

Figure 9. Changes of relative crystallinity, $x(t)$, with time during crystallization at T_c of 135 °C for PLA under the quiescent condition and different shear conditions of (a) $\dot{\gamma}$ = 1 s^{-1}, Wi_s = 2.2; (b) $\dot{\gamma}$ = 5 s^{-1}, Wi_s = 11; and (c) $\dot{\gamma}$ = 10 s^{-1}, Wi_s = 22.

found that after the undercooled PLA melt is applied to a steady shear pulse, the nucleation is remarkably accelerated, and a large number of pointlike small spherulites are observed within several minutes. It can be recognized further that the spherulites have about the same sizes for each shear conditions, indicating that the pointlike nuclei are produced at about the same time. It is generally believed that when the polymer melts are sheared, the macromolecular chains are stretched and aligned along the flow direction, and the oriented chains then assemble into parallel array and form the fibril bundles, which can behave as primary nuclei for polymer crystallization. Unlike the polymers with flexible chains such as polyethylene, PLA chains are semi-rigid and have relatively short lengths. In our case, the results do not show the row-like nuclei in PLA films, for which the applied shear rate is 10 s^{-1} (Wi_s = 22) because the shear time of 40 s (Figure 10, panel C) is still not long enough to make the PLA macromolecular chains being stretched above $\lambda^*(T)$.

Figure 10 shows that the nucleus density of undercooled PLA melt increases with increasing shear time at the shear rate of 10 s^{-1}. To well demonstrate the effects of shear on the nucleus density enhancement, typical polarized optical micrographs taken at the isothermal crystallization time of 5 min for PLA undercooled melts at different shear rates with the short and long shear times (1 s^{-1} for 5 and 45 s, 5 s^{-1} for 4 and 40 s, and 10 s^{-1} for 4 and 40 s) are shown in Figure 11. It can be

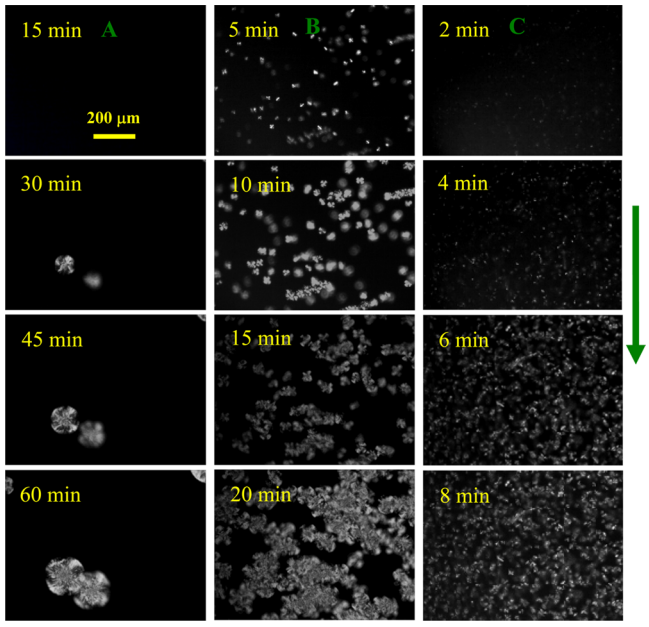

Figure 10. Selected POM micrographs for PLA during isothermal crystallization at T_c of 135 °C after being sheared at a shear rate of 10 s^{-1} for different times of (A) 0 s, (B) 4 s, and (C) 40 s. The yellow color scale bar in the top left micrograph represents 200 μm and is applied to all other micrographs. Crystallization times are indicated in the micrographs. The green color arrow on the right side of the figure indicates the shear flow direction.

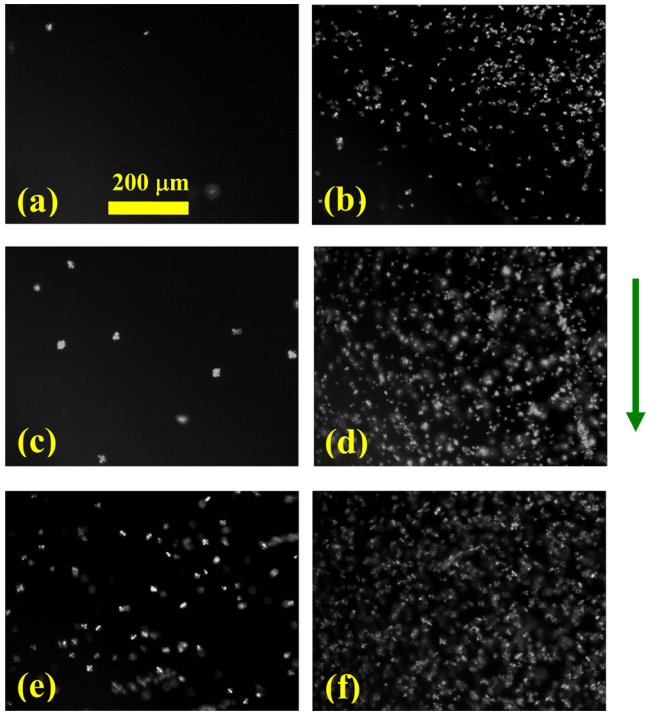

Figure 11. Selected POM micrographs for PLA during isothermal crystallization at T_c of 135 °C for 5 min after being sheared at a shear rate of 1 s^{-1} for (a) 5 s and (b) 45 s, at a shear rate of 5 s^{-1} for (c) 4 s and (d) 40 s, and at shear rate of 10 s^{-1} for (e) 4 s and (f) 40 s. The yellow color scale bar in the micrograph (a) represents 200 μm and is applied to all other micrographs. The green color arrow on the right side of the figure indicates the shear flow direction.

dx.doi.org/10.1021/sc400040b | ACS Sustainable Chem. Eng. 2013, 1, 663−672

clearly seen that the raised shear intensity subjected to the PLA undercooled melts, due to the combination of shear rate and shear time, can significantly increase the nucleus density, leading to the much fine-grained spherulitic morphology, compared with quiescent conditions (panel A in Figure 10).

Modeling Shear-Induced Isothermal Crystallization Kinetics. It has been shown in the above sections that shear flow can significantly enhance the crystallization kinetics for PLA under both the nonisothermal and isothermal crystallization conditions. The shear effects on crystallization kinetics of PLA are achieved by acceleration of the nucleation rate, which has been morphologically confirmed by the optical microscope observation. A saturation of shear effect at the longer shear times on the crystallization kinetics of PLA was observed by tracking the changes of the storage modulus with crystallization time by rheology.

In order to quantitatively evaluate the shear-induced isothermal crystallization kinetics, the Avrami model, previously used to describe the quiescent crystallization kinetics, is modified by taking into account the shear effect. This modified kinetic model proposed by Fulchiron et al.[55,58] is not able to predict the oriented crystalline morphology developed due to strong shear; however, it can provide an idea of the enhancement of the global crystallization kinetics due to a shear effect. The kinetic model for shear-induced crystallization of PLA applied in this work is summarized as follows. The effect of shear is mainly localized in the nucleation stage, as is often experimentally verified.[59] This viewpoint is also confirmed by the POM study on PLA in this work. According to the literature, the nucleation rate, $\dot{N}(t')$, can be expressed by a semi-empirical power function of shear rate, $\dot{\gamma}(t')$ by eq 6 as follows

$$\dot{N}(t') = [c\dot{\gamma}(t')]^d \tag{6}$$

where c is a constant, and d is an exponent of the power law. The total number of nuclei, N is written as the sum of the number of natural nuclei, N_0, observed at the quiescent condition and the number of activated nuclei appeared after shear treatment, N_s, which can be obtained from eq 6. The number of nuclei at the quiescent condition can be evaluated from the isothermal crystallization experiment using the Avrami equation of eq 7

$$N_0 = \frac{3K}{4\pi G^3} \tag{7}$$

where K is the Avrami crystallization rate constant, and G is the spherulite growth rate. Here, considering that an instantaneous nucleation is suitable for PLA, the Avrami exponent n can be set to 3. Furthermore, the growths of PLA spherulites are distinctively observed for the PLA samples subjected to the selected shear conditions in this work. Thus, the shear effects on the growth rates of spherulites in the undercooled PLA melts can be determined. Figure 12 shows the changes of spherulite radius as functions of time for PLA during isothermal crystallization at T_c of 135 °C after various applied shear conditions. It can be found that PLA spherulites in the sheared melts all grow linearly with time. The linearly fitted lines in Figure 12 demonstrate the same slope, indicating that the spherulitic growth rates in the sheared melts remain constant (G of 1.8 μm/min or 3.0 × 10^{-8} m/s). The absence of shear effects on the spherulitic growth rate of PLA in this work is consistent with that for shear-induced crystallization of other

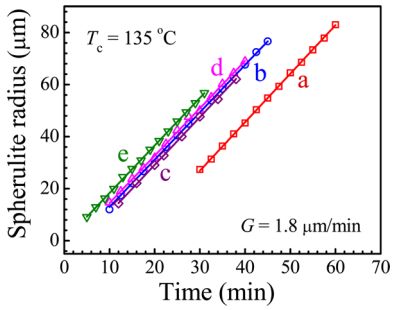

Figure 12. Changes of spherulite radius as functions of time for PLA during isothermal crystallization at T_c of 135 °C at different shear conditions: (a) quiescent condition, (b) sheared at 1 s^{-1} for 5 s, (c) sheared at 1 s^{-1} for 45 s, (d) sheared at 5 s^{-1} for 4 s, and (e) sheared at 10 s^{-1} for 4 s.

polymers.[55,60] Note that the PLA spherulites should consist of α-form lamellar crystals because the shear flow only affects the nucleus density and does not affect the subsequent spherulitic growth. The formation of α-form lamellar crystals for PLA under shear conditions has been confirmed in previous studies.[37,43] Therefore, the K value of 7.0 × 10^{-17} s^{-3} under the quiescent condition at the crystallization temperature of 135 °C can be obtained from the Avrami analysis of the $x(t)$ curve with no shear as shown in Figure 9. Then, the N_0 value of 8.8 × 10^5 m^{-3} under the quiescent condition at the crystallization temperature of 135 °C can be obtained.

On the basis of the above assumptions, the relative crystallinity, $x(t)$, taking into account of the number of extra activated nuclei due to shear, can be written as follows

$$x(t) = 1 - \exp(-\alpha') \tag{8}$$

$$\alpha' = \frac{4}{3}\pi G^3 [N_0 t^3 + \int_0^{t_s} (t - t')^3 \dot{N}(t') dt'] \tag{9}$$

where N_0 is the natural nuclei number per unit volume formed in the quiescent melt, $\dot{N}(t')$ is the nucleation rate, and t_s is the shear time. The relation between the crystallization half time, $t_{1/2}$, and shear time, t_s, can be deduced from the combination of eqs 6, 8, and 9, that is to say, $t_{1/2}$ can be obtained from eq 8 at $\alpha' = \ln(2)$. The d value of 3 was selected according to the literature.[58] The remaining unknown parameter, c, was numerically optimized to fit the decrease of the crystallization half time, $t_{1/2}$, with increasing shear time, t_s. As shown in Figure 13, the above kinetic model based on the simple but reasonable assumptions can be well applied to predict the effects of shear

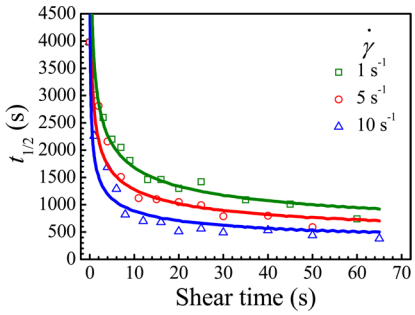

Figure 13. Changes of crystallization half time, $t_{1/2}$, as functions of shear time for PLA crystallized at T_c of 135 °C with different shear rates. Solid lines are the fitted results by the combination of eqs 6, 8, and 9.

dx.doi.org/10.1021/sc400040b | ACS Sustainable Chem. Eng. 2013, 1, 663−672

time at various shear rates on the isothermal crystallization kinetics of PLA (see the fitted solid lines in Figure 13).

CONCLUSIONS

In this study, the shear effects on the nucleation rate enhancements of PLA for both the nonisothermal and isothermal conditions were thoroughly studied by using a rotational rheometer. Prior to the shear-induced crystallization measurements, the rheological properties of PLA at the molten state were comprehensively investigated. Mastercurves of storage modulus, G', and loss modulus, $G,''$ versus the reduced angular frequency, $a_T\omega$, for PLA at the reference temperature of 190 °C were successfully constructed by applying the time−temperature superposition principle. The critical shear rates for the orientation and stretch of the longest chains (high molecular mass tails) of PLA at the temperature of 135 °C were determined to be 0.0076 and 0.45 s^{-1}, respectively. In the followed shear-induced crystallization measurements, the shear rates were set as high to guarantee that the stretch of the longest chains (high molecular mass tails) of PLA was expected. It was found that the crystallization process under shear was greatly enhanced compared to the quiescent conditions, and the crystallization kinetics was accelerated with the increases in shear rate and/or shear time. For a certain shear rate, a critical shear time existed, and a further increase in shear time did not lead to a further acceleration of the crystallization process. In situ POM observations demonstrated the enhanced nuclei density under application of shear and the constant spherulitic growth rates, demonstrating that the effects of shear on acceleration of PLA crystallization kinetics were achieved mainly through the enhancements of nucleation. The effects of shear rate and shear time on the enhanced crystallization kinetics of PLA could be successfully evaluated by using a kinetic model based on directly relating the extra number of activated nuclei created during shear to the shear rate.

AUTHOR INFORMATION

Corresponding Author

*Tel.: +86 0551-63607703. Fax: +86 0551-63607703. E-mail: zgwang2@ustc.edu.cn.

Author Contributions

Yong Zhong and Huagao Fang have equal contribution to this work.

Notes

The authors declare no competing financial interest.

ACKNOWLEDGMENTS

Z.G. Wang acknowledges the financial support from the National Science Foundation of China with Grant No. 21174139 and National Basic Research Program of China with Grant No. 2012CB025901.

REFERENCES

(1) Ikada, Y.; Tsuji, H. Biodegradable polyesters for medical and ecological applications. *Macromol. Rapid Commun.* **2000**, *21*, 117−132.
(2) Drumright, R. E.; Gruber, P. R.; Henton, D. E. Polylactic acid technology. *Adv. Mater.* **2000**, *12*, 1841−1846.
(3) Bogaert, J. C.; Coszach, P. Poly(lactic acids): A potential solution to plastic waste dilemma. *Macromol. Symp.* **2000**, *153*, 287−303.
(4) Garlotta, D. A literature review of poly(lactic acid). *J. Polym. Environ.* **2001**, *9*, 63−84.
(5) Odelius, K.; Hoglund, A.; Kumar, S.; Hakkarainen, M.; Ghosh, A. K.; Bhatnagar, N.; Albertsson, A. C. Porosity and pore size regulate the degradation product profile of polylactide. *Biomacromolecules* **2011**, *12*, 1250−1258.
(6) Numata, K.; Finne-Wistrand, A.; Albertsson, A. C.; Doi, Y.; Abe, H. Enzymatic degradation of monolayer for poly(lactide) revealed by real-time atomic force microscopy: Effects of stereochemical structure, molecular weight, and molecular branches on hydrolysis rates. *Biomacromolecules* **2008**, *9*, 2180−2185.
(7) Tsuji, H.; Miyauchi, S. Enzymatic hydrolysis of poly(lactide)s: Effects of molecular weight, L-lactide content, and enantiomeric and diastereoisomeric polymer blending. *Biomacromolecules* **2001**, *2*, 597−604.
(8) Rasal, R. M.; Janorkar, A. V.; Hirt, D. E. Poly(lactic acid) modifications. *Prog. Polym. Sci.* **2010**, *35*, 338−356.
(9) Hoglund, A.; Hakkarainen, M.; Edlund, U.; Albertsson, A. C. Surface modification changes the degradation process and degradation product pattern of Polylactide. *Langmuir* **2010**, *26*, 378−383.
(10) Lim, L. T.; Auras, R.; Rubino, M. Processing technologies for poly(lactic acid). *Prog. Polym. Sci.* **2008**, *33*, 820−852.
(11) Di Lorenzo, M. L. Crystallization behavior of poly(L-lactic acid). *Eur. Polym. J.* **2005**, *41*, 569−575.
(12) Bhardwaj, R.; Mohanty, A. K. Modification of brittle polylactide by novel hyperbranched polymer-based nanostructures. *Biomacromolecules* **2007**, *8*, 2476−2484.
(13) Liu, H. Z.; Song, W. J.; Chen, F.; Guo, L.; Zhang, J. W. Interaction of microstructure and interfacial adhesion on impact performance of polylactide (PLA) ternary blends. *Macromolecules* **2011**, *44*, 1513−1522.
(14) Pan, P. J.; Zhu, B.; Inoue, Y. Enthalpy relaxation and embrittlement of poly(L-lactide) during physical aging. *Macromolecules* **2007**, *40*, 9664−9671.
(15) Ljungberg, N.; Wesslen, B. Preparation and properties of plasticized poly(lactic acid) films. *Biomacromolecules* **2005**, *6*, 1789−1796.
(16) Tsuji, H.; Ikada, Y. Blends of isotactic and atactic poly(lactide)s. 2. Molecular-weight effects of atactic component on crystallization and morphology of equimolar blends from the melt. *Polymer* **1996**, *37*, 595−602.
(17) Miyata, T.; Masuko, T. Morphology of poly(L-lactide) solution-grown crystals. *Polymer* **1997**, *38*, 4003−4009.
(18) Pan, P.; Liang, Z.; Zhu, B.; Dong, T.; Inoue, Y. Roles of physical aging on crystallization kinetics and induction period of poly(L-lactide). *Macromolecules* **2008**, *41*, 8011−8019.
(19) Abe, H.; Kikkawa, Y.; Inoue, Y.; Doi, Y. Morphological and kinetic analyses of regime transition for poly[(s)-lactide] crystal growth. *Biomacromolecules* **2001**, *2*, 1007−1014.
(20) Zhang, J.; Tashiro, K.; Tsuji, H.; Domb, A. J. Disorder-to-order phase transition and multiple melting behavior of poly(L-lactide) investigated by simultaneous measurements of WAXD and DSC. *Macromolecules* **2008**, *41*, 1352−1357.
(21) Kawai, T.; Rahman, N.; Matsuba, G.; Nishida, K.; Kanaya, T.; Nakano, M.; Okamoto, H.; Kawada, J.; Usuki, A.; Honma, N.; Nakajima, K.; Matsuda, M. Crystallization and melting behavior of poly(L-lactic acid). *Macromolecules* **2007**, *40*, 9463−9469.
(22) Tsuji, H.; Miyase, T.; Tezuka, Y.; Saha, S. K. Physical properties, crystallization, and spherulite growth of linear and 3-arm poly(L-lactide)s. *Biomacromolecules* **2005**, *6*, 244−254.
(23) Zhang, J. M.; Tsuji, H.; Noda, I.; Ozaki, Y. Structural changes and crystallization dynamics of poly(L-lactide) during the cold-crystallization process investigated by infrared and two-dimensional infrared correlation spectroscopy. *Macromolecules* **2004**, *37*, 6433−6439.
(24) Balzano, L.; Kukalyekar, N.; Rastogi, S.; Peters, G. W. M.; Chadwick, J. C. Crystallization and dissolution of flow-induced precursors. *Phys. Rev. Lett.* **2008**, *100*, 048302.
(25) Balzano, L.; Rastogi, S.; Peters, G. Self-nucleation of polymers with flow: The case of bimodal polyethylene. *Macromolecules* **2011**, *44*, 2926−2933.

(26) Phillips, A. W.; Bhatia, A.; Zhu, P. W.; Edward, G. Shish formation and relaxation in sheared isotactic polypropylene containing nucleating particles. *Macromolecules* **2011**, *44*, 3517−3528.
(27) Mykhaylyk, O. O.; Chambon, P.; Impradice, C.; Fairclough, J. P. A.; Terrill, N. J.; Ryan, A. J. Control of structural morphology in shear-induced crystallization of polymers. *Macromolecules* **2010**, *43*, 2389−2405.
(28) Ma, Z.; Balzano, L.; Peters, G. W. M. Pressure quench of flow-induced crystallization precursors. *Macromolecules* **2012**, *45*, 4216−4224.
(29) Cavallo, D.; Azzurri, F.; Balzano, L.; Funari, S. S.; Alfonso, G. C. Flow memory and stability of shear-induced nucleation precursors in isotactic polypropylene. *Macromolecules* **2010**, *43*, 9394−9400.
(30) Keum, J. K.; Zuo, F.; Hsiao, B. S. Formation and stability of shear-induced shish-kebab structure in highly entangled melts of UHMWPE/HDPE blends. *Macromolecules* **2008**, *41*, 4766−4776.
(31) Van der Beek, M. H. E.; Peters, G. W. M.; Meijer, H. E. H. Classifying the combined influence of shear rate, temperature, and pressure on crystalline morphology and specific volume of isotactic polypropylene. *Macromolecules* **2006**, *39*, 9278−9284.
(32) Somani, R. H.; Yang, L.; Hsiao, B. S.; Sun, T.; Pogodina, N. V.; Lustiger, A. Shear-induced molecular orientation and crystallization in isotactic polypropylene: Effects of the deformation rate and strain. *Macromolecules* **2005**, *38*, 1244−1255.
(33) Kumaraswamy, G.; Verma, R. K.; Kornfield, J. A.; Yeh, F. J.; Hsiao, B. S. Shear-enhanced crystallization in isotactic polypropylene. In-situ synchrotron SAXS and WAXD. *Macromolecules* **2004**, *37*, 9005−9017.
(34) Kumaraswamy, G.; Issaian, A. M.; Kornfield, J. A. Shear-enhanced crystallization in isotactic polypropylene. 1. Correspondence between in situ rheo-optics and ex situ structure determination. *Macromolecules* **1999**, *32*, 7537−7547.
(35) Tang, H.; Chen, J. B.; Wang, Y.; Xu, J. Z.; Hsiao, B. S.; Zhong, G. J.; Li, Z. M. Shear flow and carbon nanotubes synergistically induced nonisothermal crystallization of poly(lactic acid) and its application in injection molding. *Biomacromolecules* **2012**, *13*, 3858−3867.
(36) Fitz, B. D.; Jamiolkowski, D. D.; Andjelić, S. Tg depression in poly(L-lactide) crystallized under partially constrained conditions. *Macromolecules* **2002**, *35*, 5869−5872.
(37) Mahendrasingam, A.; Blundell, D. J.; Parton, M.; Wright, A. K.; Rasburn, J.; Narayanan, T.; Fuller, W. Time resolved study of oriented crystallisation of poly(lactic acid) during rapid tensile deformation. *Polymer* **2005**, *46*, 6009−6015.
(38) Cicero, J. A.; Dorgan, J. R.; Janzen, J.; Garrett, J.; Runt, J.; Lin, J. S. Supramolecular morphology of two-step, melt-spun poly(lactic acid) fibers. *J. Appl. Polym. Sci.* **2002**, *86*, 2828−2838.
(39) Cicero, J. A.; Dorgan, J. R.; Garrett, J.; Runt, J.; Lin, J. S. Effects of molecular architecture on two-step, melt-spun poly(lactic acid) fibers. *J. Appl. Polym. Sci.* **2002**, *86*, 2839−2846.
(40) Li, X. J.; Li, Z. M.; Zhong, G. J.; Li, L. B. Steady-shear-induced isothermal crystallization of poly(L-lactide) (PLLA). *J. Macromol. Sci., Phys.* **2008**, *47*, 511−522.
(41) Li, X. J.; Zhong, G. J.; Li, Z. M. Non-isothermal crystallization of poly(L-lactide) (PLLA) under quiescent and steady shear conditions. *Chin. J. Polym. Sci.* **2010**, *28*, 357−366.
(42) Yamazaki, S.; Itoh, M.; Oka, T.; Kimura, K. Formation and morphology of "shish-like" fibril crystals of aliphatic polyesters from the sheared melt. *Eur. Polym. J.* **2010**, *46*, 58−68.
(43) Huang, S. Y.; Li, H. F.; Jiang, S. C.; Chen, X. S.; An, L. J. Crystal structure and morphology influenced by shear effect of poly(L-lactide) and its melting behavior revealed by WAXD, DSC and in-situ POM. *Polymer* **2011**, *52*, 3478−3487.
(44) Meerveld, J.; Peters, G. W. M.; Hutter, M. Towards a rheological classification of flow induced crystallization experiments of polymer melts. *Rheol. Acta* **2004**, *44*, 119−134.
(45) Palade, L.-I.; Lehermeier, H. J.; Dorgan, J. R. Melt rheology of high L-content poly(lactic acid). *Macromolecules* **2001**, *34*, 1384−1390.
(46) Cooper-White, J. J.; Mackay, M. E. Rheological properties of poly(lactides). Effect of molecular weight and temperature on the viscoelasticity of poly(L-lactic acid). *J. Polym. Sci., Part B: Polym. Phys.* **1999**, *37*, 1803−1814.
(47) Maosko, C. W. *Rheology, Principles, Measurements and Applications*; Wiley-VCH: New York, 1994.
(48) Housmans, J.-W.; Steenbakkers, R. J. A.; Roozemond, P. C.; Peters, G. W. M.; Meijer, H. E. H. Saturation of pointlike nuclei and the transition to oriented structures in flow-induced crystallization of isotactic polypropylene. *Macromolecules* **2009**, *42*, 5728−5740.
(49) Vleeshouwers, S.; Meijer, H. E. H. A rheological study of shear induced crystallization. *Rheol. Acta* **1996**, *35*, 391−399.
(50) Lagasse, R. R.; Maxwell, B. Experimental-study of kinetics of polymer crystallization during shear-flow. *Polym. Eng. Sci.* **1976**, *16*, 189−199.
(51) Seki, M.; Thurman, D. W.; Oberhauser, J. P.; Kornfield, J. A. Shear-mediated crystallization of isotactic polypropylene: The role of long chain-long chain overlap. *Macromolecules* **2002**, *35*, 2583−2594.
(52) Azzurri, F.; Alfonso, G. C. Insights into formation and relaxation of shear-induced nucleation precursors in isotactic polystyrene. *Macromolecules* **2008**, *41*, 1377−1383.
(53) Doi, M.; Edwards, S. F. *The Theory of Polymer Dynamics*; Clarendon Press: Oxford, 1986.
(54) Mechbal, N.; Bousmina, M. Uniaxial deformation and relaxation of polymer blends: Relationship between flow and morphology development. *Rheol. Acta* **2004**, *43*, 119−126.
(55) Koscher, E.; Fulchiron, R. Influence of shear on polypropylene crystallization: Morphology development and kinetics. *Polymer* **2002**, *43*, 6931−6942.
(56) Vega, J.; Hristova, D.; Peters, G. Flow-induced crystallization regimes and rheology of isotactic polypropylene. *J. Therm. Anal. Calorim.* **2009**, *98*, 655−666.
(57) Pogodina, N. V.; Winter, H. H.; Srinivas, S. Strain effects on physical gelation of crystallizing isotactic polypropylene. *J. Polym. Sci., Part B: Polym. Phys.* **1999**, *37*, 3512−3519.
(58) Naudy, S.; David, L.; Rochas, C.; Fulchiron, R. Shear induced crystallization of poly(m-xylylene adipamide) with and without nucleating additives. *Polymer* **2007**, *48*, 3273−3285.
(59) Acierno, S.; Grizzuti, N. Flow-induced crystallization of polymer: Theory and experiments. *Int. J. Mater. Form* **2008**, *1*, 583−586.
(60) Abuzaina, F. M.; Fitz, B. D.; Andjelić, S.; Jamiolkowski, D. D. Time resolved study of shear-induced crystallization of poly(p-dioxanone) polymers under low-shear, nucleation-enhancing shear conditions by small angle light scattering and optical microscopy. *Polymer* **2002**, *43*, 4699−4708.